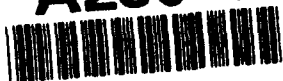


**Best
Available
Copy**

AD-A280 634



ARMY RESEARCH LABORATORY



**EVAPORATION AND THE SOIL MOISTURE
AVAILABILITY COEFFICIENT**

Frank V. Hansen

ARL-TR-263

March 1994



DTIC QUALITY INSPECTED 8

94-19348



Approved for public release; distribution is unlimited.

94 6 23 150

NOTICES

Disclaimers

The findings in this report are not to be construed as an official Department of the Army position, unless so designated by other authorized documents.

The citation of trade names and names of manufacturers in this report is not to be construed as official Government indorsement or approval of commercial products or services referenced herein.

Destruction Notice

When this document is no longer needed, destroy it by any method that will prevent disclosure of its contents or reconstruction of the document.

REPORT DOCUMENTATION PAGE			Form Approved OMB No. 0704-0188	
Public reporting burden for this collection of information is estimated to average 1 hour per response, including the time for reviewing instructions, searching existing data sources, gathering and maintaining the data needed, and completing and reviewing the collection of information. Send comments regarding this burden estimate or any other aspect of this collection of information, including suggestions for reducing this burden, to Washington Headquarters Services, Directorate for Information Operations and Reports, 1215 Jefferson Davis Highway, Suite 1204, Arlington, VA 22202-4302, and to the Office of Management and Budget, Paperwork Reduction Project (0704-0188), Washington, DC 20503				
1. AGENCY USE ONLY (Leave blank)	2. REPORT DATE March 1994	3. REPORT TYPE AND DATES COVERED Final		
4. TITLE AND SUBTITLE EVAPORATION AND THE SOIL MOISTURE AVAILABILITY COEFFICIENT		5. FUNDING NUMBERS		
6. AUTHOR(S) Frank V. Hansen				
7. PERFORMING ORGANIZATION NAME(S) AND ADDRESS(ES) U.S. Army Research Laboratory Battlefield Environment Directorate ATTN: AMSRL-BE-W White Sands Missile Range, NM 88002-5501		8. PERFORMING ORGANIZATION REPORT NUMBER ARL-TR-263		
9. SPONSORING/MONITORING AGENCY NAME(S) AND ADDRESS(ES) U.S. Army Research Laboratory 2800 Powder Mill Road Adelphi, MD 20783-1145		10. SPONSORING/MONITORING AGENCY REPORT NUMBER		
11. SUPPLEMENTARY NOTES				
12a. DISTRIBUTION/AVAILABILITY STATEMENT Approved for public release; distribution is unlimited.		12b. DISTRIBUTION CODE		
13. ABSTRACT (Maximum 200 words) Evaporative processes at the air-earth interface are examined in terms of a moisture availability coefficient. A postulate is formed for developing the availability coefficient utilizing the ratio of potential evaporation to actual evaporation. Experimental data is used to evaluate this approach and results indicate that the moisture availability coefficient appears to be independent of climate, season of the year or latitude and soil type. A preliminary study of the effects of atmospheric water vapor on the dynamic stability of the surface boundary layer was also undertaken.				
14. SUBJECT TERMS Evaporation, evapotranspiration, similarity theory, Obukhov scaling length, water vapor, specific humidities			15. NUMBER OF PAGES 19	
			16. PRICE CODE	
17. SECURITY CLASSIFICATION OF REPORT Unclassified	18. SECURITY CLASSIFICATION OF THIS PAGE Unclassified	19. SECURITY CLASSIFICATION OF ABSTRACT Unclassified	20. LIMITATION OF ABSTRACT SAR	

Contents

List of Illustrations	4
1. Introduction	5
2. Background	5
3. Evaporation	8
4. Discussion	10
5. Conclusions	13
References	17
Distribution List	19

Accession For	
NTIS GRA&I	<input checked="" type="checkbox"/>
DTIC TAB	<input type="checkbox"/>
Unannounced	<input type="checkbox"/>
Justification	
By _____	
Distribution/ _____	
Availability Codes	
Dist	Avail and/or Special
A-1	

List of Illustrations

Tables

1. The Surface Energy Balance and Atmospheric Stability as a
Function of Relative Humidity 12

Figures

1. The temperature dependence of the square root of time coefficient (open circles)
and of the water vapor diffusion in soil (line) 14
2. The moisture availability coefficient evaluated using evaporation data from the
African Sahel, central Texas, and southern Arizona 15
3. A comparison of equations (21) and (22) in terms of the scaling ratio Z/L 16

1. Introduction

Water vapor in the atmosphere may be considered as originating from two sources: evaporation from the water surface associated with the volumetric water content of the soil and the molecular diffusion of vapor from the remainder of the soil pores. The water vapor content of the atmosphere must be considered when dealing with atmospheric processes involving the turbulent kinetic energy budget or the surface energy balance. Specifically, when dealing with buoyant heat fluxes in the surface boundary layer, the portion of the energy contributed by the latent heat flux must be accurately determined; otherwise, uncertainties will occur in subsequent calculations.

Evaporation from a bare surface or evapotranspiration from a vegetated surface is a function of soil types, soil heat fluxes, net radiation, volumetric water content of the soil, and the time since natural or artificial irrigation ended. Natural irrigation may be defined as precipitation. Parameterization of the static or dynamic structure of the surface boundary layer of the atmosphere can be accomplished by using semiempirical or engineering estimate approaches. These techniques can be based upon much simplified and modified forms of the Penman (1948) potential evaporation equation, which can be combined with the dynamic similarity of flows theory of Obukhov (1946).

2. Background

Semiempirical parameterization and amplification of any scheme leading to practical engineering estimates of atmospheric surface boundary layer processes require some clarification and the tying together of some seemingly unrelated principles. A primary assumption, based upon the work of Brunner (1977), is that the relative humidity is constant with height in the first 100 or so meters of the atmosphere. This premise allows specific humidity and vapor pressure profiles to be established from wet- and dry-bulb temperature measurements at one level above the surface.

The saturation vapor pressure e_s can be calculated for any temperature T at any height z using Tetens's (1930) formula in the modified form

$$e_s = 6.11 \exp \left[\frac{17.4(T - 273.16)}{T - 34.16} \right] \quad (1)$$

where T is in degrees kelvin.

If the relative humidity is known, then the ambient vapor pressure is found from

$$e = e_s (RH) \quad (2)$$

where RH is the relative humidity. Specific humidities are determined from

$$q = 0.621 \frac{e}{p - 0.379e} \quad (3)$$

where p is atmospheric pressure in millibars. The density of moist air may be found from

$$\rho_w = \frac{P}{R\theta_v} \quad (4)$$

where R is the gas constant and θ_v the virtual potential temperature given by

$$\theta_v = \frac{\theta}{1 - 0.379e/P} \quad (5)$$

Actual evaporation rates influence not only the latent heat flux into the atmosphere, but also buoyancy, dynamic stability and, of course, the specific humidity profile, which is typically written as

$$\frac{q^*}{k} = \frac{q - q_o}{\ln \frac{z}{z_o} + \psi_B \left(\frac{z}{L} \right)} \quad (6)$$

when q^* is a scaling humidity, k is Karman's constant, q specific humidity, q_0 the specific humidity at z_0 , the surface roughness length, z height and $\psi_H(z/L)$ the diabatic influence function for heat. In the Obukhov (1946) similarity theory, heat and mass transfer are taken to be identical, hence the use of $\psi_H(z/L)$ for moisture profiles. According to Myrup's (1969) semiempirical results,

$$q_0 = \frac{RH}{1000} \left[3.74 + 2.67 \left(\frac{T_0}{10} \right)^2 \right] \quad (7)$$

where T_0 is the temperature at z_0 in degrees Celsius.

The surface energy balance is usually written in the form

$$R_N = H + L E + G \quad (8)$$

where R_N is the net radiation, H the sensible heat flux, LE the latent heat flux and G the soil heat flux. The sensible heat flux with respect to the eddy diffusivity is given by

$$H = -c_p K_H \frac{\partial \bar{\theta}}{\partial z} \quad (9)$$

where C_p is the specific heat of air at constant pressure ($c_p = 1014 \text{ J kg}^{-1} \text{ }^\circ\text{K}^{-1}$), ρ density, K_H the eddy diffusivity and θ potential temperature. Equation (9) can also be written in terms of U and T^* as

$$H = -c_p \rho u_* T^* \quad (10)$$

or

$$H = -C_p \rho_w u_* \theta_v^* \quad (11)$$

where u_* is the friction velocity, T^* a scaling temperature and θ_* a virtual scaling temperature.

Similarly, the latent heat flux (LE) is given by

$$L E = - \rho L u_* q_* \quad (12)$$

where L is the latent heat of vaporization and E the evaporation rate. The buoyant heat flux is now written as

$$H' = (H + 0.07 L E) \quad (13)$$

3. Evaporation

The release of water vapor from the soil to the atmosphere can be thought of as bare surface evaporation and evapotranspiration from vegetated surface and is a most complex boundary layer phenomenon. According to Penman (1948) the potential latent heat flux can be shown to be

$$L E_p = \frac{S}{S + \sigma} (R_n - G) + \frac{\sigma}{S + \sigma} (e_s - e_d) f(\bar{v}) \quad (14)$$

where S is the slope of the saturation specific humidity curve versus temperature, σ is the psychrometric constant, e_s is the saturation vapor pressure for ambient air, e_d is the saturation vapor pressure at the dew point, and $f(\bar{v})$ is a function of the horizontal mean wind speed \bar{v} , given by

$$f(\bar{v}) = 0.35 \left(1 + \frac{\bar{v}}{100} \right) \quad (15)$$

over a grassy surface.

To establish the actual evaporation a moisture availability coefficient M such as suggested by Nappo (1975) may be written as the ratio of actual evaporation to potential evaporation given by

$$M = E/E_p \quad (16)$$

Jackson, Idso, and Reginato (1976) were able to express M in terms of the increasing albedo of drying soils, as

$$M = (\alpha_d - \alpha)/(\alpha_d - \alpha_w) \quad (17)$$

where α_d is the dry soil albedo, α_w is wet soil albedo, and α is the albedo for a particular time. Albedo measurements were also found to be an ideal mechanism of integrating various drying ratios and partitioning the portions contributing to the energy limiting, or potential evaporation, and the soil limiting phases of the process. The coefficient M will vary from unity for a soil at field capacity to zero for a dry surface. The potential evaporation rate can be combined with the soil limiting rate E_s to obtain the actual evaporation ratio.

$$E = M E_p + (1 - M) E_s \quad (18)$$

Ritchie (1972) found the soil limiting rate to be

$$E_s = C t^{-1/2} \quad (19)$$

where t is the time in days and c varies with soil type and season of the year. Seasonal dependencies are a function of temperature and will vary by about a factor of 2 from winter to summer as shown in figure 1.

The complexity of the evaporation process requires that the energy limiting and soil limiting phases be partitioned according to the starting times of the soil limiting fraction. Thus, equation (18) must be rewritten as

$$E = M E_p + C \sum (M_{i_1} - M_i) (n - i + 1)^{-1/2} \quad (20)$$

where n is the number of days after evaporation began. Multiplying both sides of equation (20) by L yields the latent heat flux.

The moisture availability coefficient M has been evaluated using evaporation data extracted from Dugdale (1989), Ritchie (1972), and Jackson (1973). Potential evaporation E_p was taken to be the evaporation rate on day 1 after irrigation or rainfall ended and used as the numerator in equation (16) for normalizing the data. The three data samples were from widely different climatic regions (Southern Arizona, Central Texas, and the African Sahel) and it is noteworthy that when normalized a single curve fits all the data quite well, as shown in figure 2.

Dugdale's data were for three separate rainfall amounts, 3, 7.5, and 15 mm; while the Jackson et al. (1976) samples were for all four seasons of the year. Ritchie's data were for four soil types (Adalanto Clay Loam, Yolo Loam, Houston Black Clay and Plainfield sand). These results although not definitive suggest that, discounting extremes such as Jackson's summertime evaporation rates and the one very light rainfall (3 mm) reported by Dugdale, the coefficient M may well be independent of season, rainfall amounts, and soil type.

4. Discussion

The importance of considering evaporative processes and the evaluation of specific humidity profiles in the surface boundary layer significantly concerns water vapor effects upon the dynamic stability of the atmosphere and the surface energy balance. Atmospheric stability in the surface boundary layer is generally designated by the Obukhov (1946) length, and according to Busch (1973) is given by

$$L = \frac{u_*^2 \bar{\theta}_v}{kg\theta^*} \quad (21)$$

where g is the gravitational acceleration.

Richardson (1920) and Obukhov initially ignored the contribution of latent heat to buoyancy, and consequently, the accepted similarity definitions of

$$\frac{z}{L} = - \frac{kgzH}{u_*^3 c_p \rho \theta} = R_i \phi_m \frac{K_H}{K_m} = R_i \frac{\phi_H}{\phi_m^2} \quad (22)$$

where ϕ_H and ϕ_m are dimensionless lapse rates and wind shears respectively and K_m is the eddy viscosity (only valid in totally dry air).

Figure 3 shows a comparison of equations (21) and (22) in terms of the scaling ratio z/L . The data utilized to prepare figure 3 was extracted from a compilation by Barad (1958) of wind, temperature, and vapor pressure profiles observed during Project Prairie Grass. These data were carefully screened and 12 reasonably stationary and homogeneous profiles were selected for analysis. Note in figure 3 that the exclusion of water vapor in equation (22) indicates an atmosphere less stable than it really is.

The surface energy balance, as given by equation (8), is also dramatically modified by an increase in atmospheric water vapor. Two simulated cases are given in table 1 for relative humidities of 25 and 75 percent. Initial conditions are presumed to be identical with the exception of the relative humidity. Tripling the relative humidity drastically alters the surface energy balance as a function of incoming solar radiation reaching the earth's surface. Insolation is reduced by 33 W m^{-2} or about 4 percent, while the net radiation increases by approximately 4 percent. The most significant modification to the surface boundary layer occurs in the stability parameters L and z/L , both of which decrease by 37 percent. This decrease is attributed to the approximately 17 percent increase in the latent heat flux and an extremely large, 43 percent, decrease in buoyant heat flux. The results show that atmospheric water vapor, or evapotranspiration, cannot be ignored in the surface boundary layer.

The increase of water vapor in the atmosphere resulting from the increase in the relative humidity has the effect of reducing the transparency to radiation, especially the visible radiation. The presence of water vapor as a suspensoid will account for the indicated changes in the surface energy balance.

Table 1. The Surface Energy Balance and Atmospheric Stability as a Function of Relative Humidity

Parameter	RH = 25 %	RH = 75 %
Height	2 m	2 m
Roughness length	0.0065 m	0.0065 m
Temperature	27 °C	27 °C
Wind speed	4 m s ⁻¹	4 m s ⁻¹
Insolation	875 W m ⁻²	842 W m ⁻²
Net radiation	675 W m ⁻²	740 W m ⁻²
Soil heat flux	66 W m ⁻²	141 W m ⁻²
Sensible heat flux	249 W m ⁻²	127 W m ⁻²
Latent heat flux	363 W m ⁻²	436 W m ⁻²
Buoyant heat flux	275 W m ⁻²	158 W m ⁻²
Scaling temperature	-0.9664	-0.5078
Virtual scaling temperature	-1.07	-0.635
Obukhov length	-3.52 m	-5.63 m
Scaling ratio	-0.5683	-0.3551

The simulation of the table was performed by using a surface energy balance model developed by Rachele and Tunick (1991).

The moisture availability coefficient illustrated in figure 2, determined from experimental data, appears to be a valid approach for weighing the potential evaporation as a means for estimating actual evaporation. These preliminary results need to be expanded to include correlations between daily normalized evaporation rates and the mean daily volumetric water content of the soil. Other verification techniques involving the obvious relationships between evaporation versus season, soil type, latitude and climatic extremes are obviously needed.

The determination of the latent heat flux using equation (12) yields values equivalent to the potential latent heat flux (equation (14)), indicating that the moisture availability coefficient (equation (16)) must be added to equation (12), such that

$$L E = - M L \rho u_s q_s \quad (23)$$

resulting in an expression for the actual latent heat flux.

5. Conclusions

The impact of evaporation and the presence of water vapor in the atmosphere have an almost arcane effect upon the observed dynamics of the surface boundary layer. The addition of moisture to surface boundary layer models such as the dynamic similarity theory is in reality quite simple, especially if the moisture availability coefficient approach is used. The apparently almost independent nature of the coefficient in its normalized form is considered to be a valuable asset to the modeling of atmospheric processes. As additional experimental data becomes available, further exploration and exploitation of the moisture availability coefficient will be undertaken.

$$E = ME_p + (1 - M) E_s . \quad (24)$$

Ritchie (1972) found the soil limiting rate to be

$$E_s = C t^{-1/2}, \quad (25)$$

where t is time in days and C varies with soil type and season of the year. Seasonal dependencies are a function of temperature and will vary by about a factor of 2 from winter to summer as shown in figure 1. Moisture availability coefficients extracted from Jackson et al. (1976) are given in figure 2.

The complexity of the evaporation process requires that the energy limiting and soil limiting phases be partitioned according to the starting times of the soil limiting fraction. Thus equation (17) must be rewritten as

$$E = ME_p + C \sum (M_{i-1} - M_i) (n - i + 1)^{-1/2}, \quad (26)$$

where n is the number of days after evaporation began.

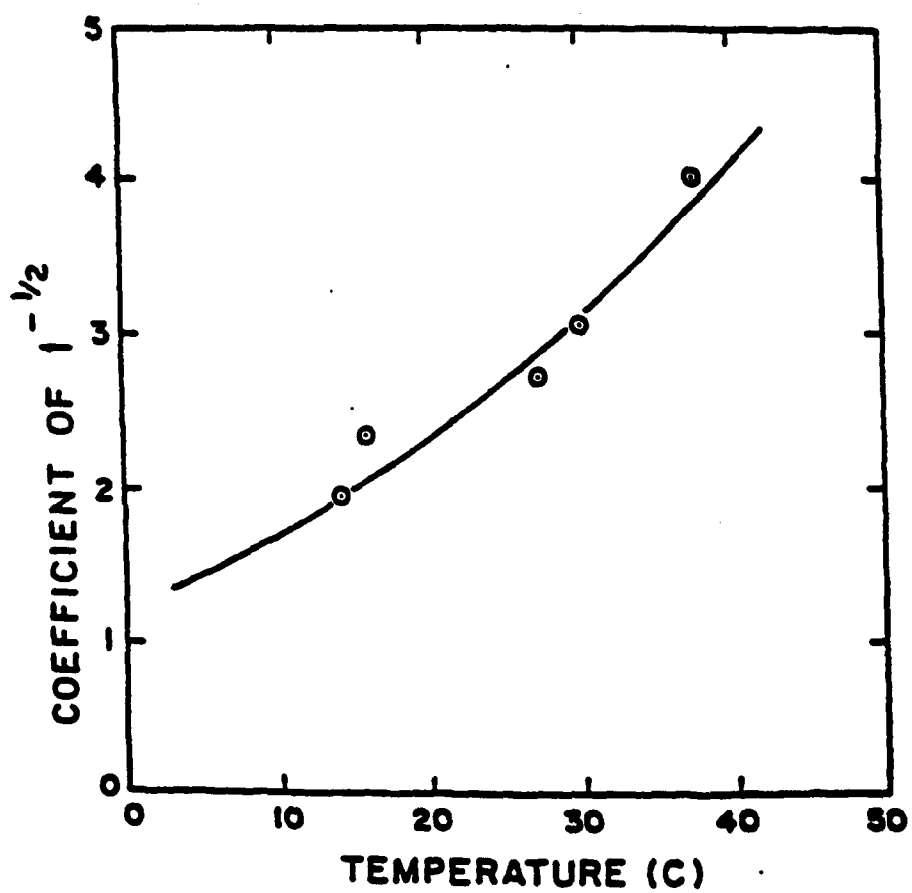


Figure 1. The temperature dependence of the square root of time coefficient (open circles) and of the water vapor diffusion in soil (line).

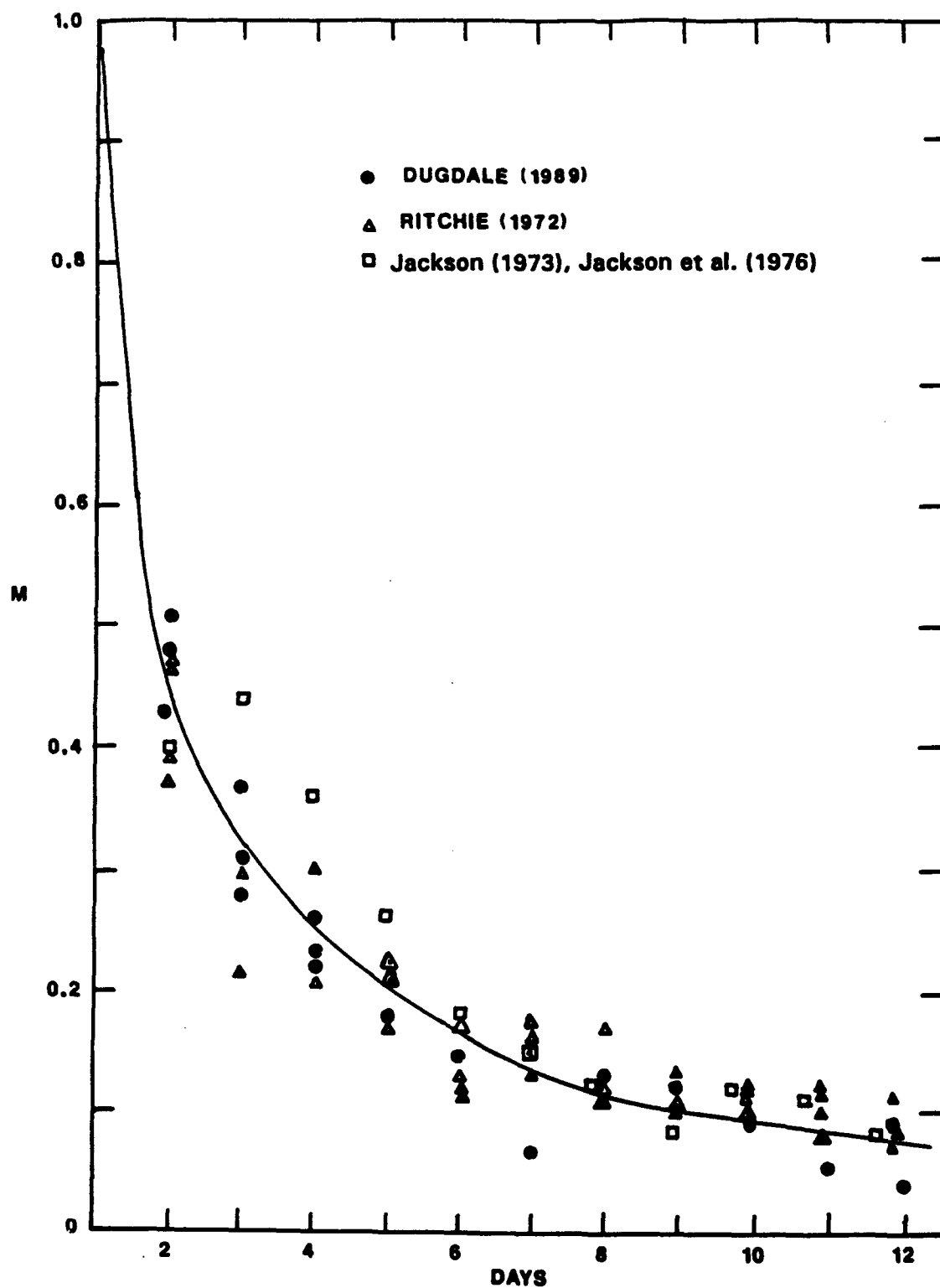


Figure 2. The moisture availability coefficient evaluated using evaporation data from the African Sahel, central Texas, and southern Arizona.

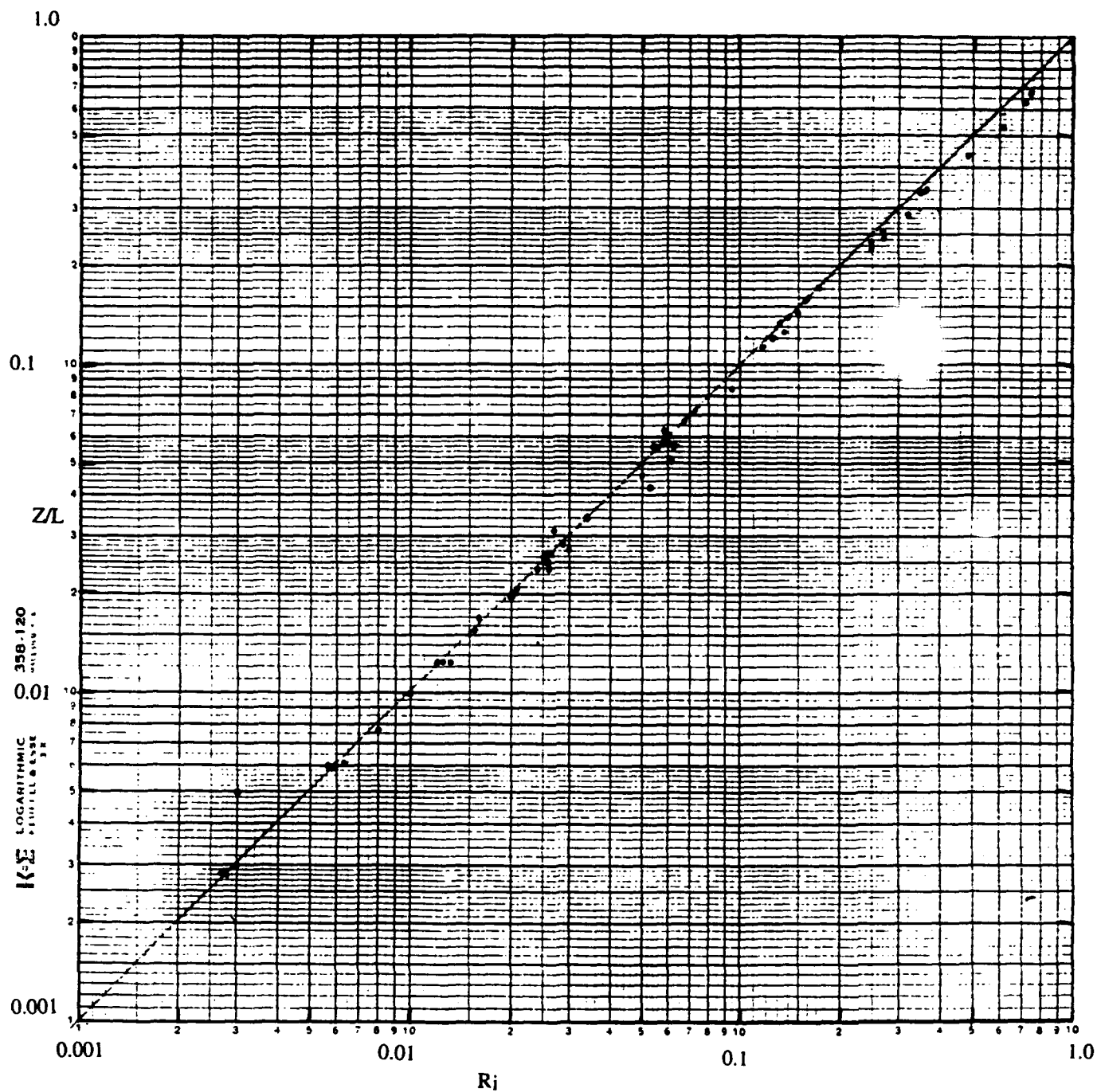


Figure 3. A comparison of equations (21) and (22) in terms of the scaling ratio Z/L .

References

- Barad, M. L., 1958, Project Prairie Grass. A Field Program in Diffusion. Vol II. AFCRL-TR-58-235 (II), Air Force Cambridge Research Center, Bedford, MA.
- Brunner, F. K., 1977, On the Refraction Coefficient of Microwaves, Bull Geol. 51:257-264.
- Busch, N. E., 1973, "On the Mechanics of Atmospheric Turbulence" in Workshop of Micrometeorology (D.A. Haugen, ed) American Meteorological Society, Boston, MA, pp 1-61.
- Dugdale, G., 1989, The Influence of Variability of Rainfall and Soil Moisture on Evaporation From Semi-arid Areas. University of Reading, Reading, U.K.
- Jackson, R. D., 1973, Diurnal Changes in Soil Water Content During Drying. Field Water Regime Special Pub No. 5, In Proceedings, Soil Science Society of America.
- Jackson, R. D., S. B. Idso, and R. J. Reginato, 1976, Calculation of Evaporation Rates During the Transition from Energy Limiting to Soil-limiting Phases Using Albedo Data. Water Res. Resch. 12(1):23-26.
- Myrup, L. O., 1969, A Numerical Model of the Urban Heat Island, J Appl Meteorol. 8:908-918.
- Nappo, C. J., Jr., 1975, Parameterization of Surface Moisture and Evaporation Rate in a Planetary Boundary Layer Model. J Appl Meteorol. 14:289-296.
- Obukhov, A. M., 1946, Turbulence in an Atmosphere of Nonhomogeneous Temperature. Trans Inst Theort Geophys USSR. 1:95.
- Penman, H. L., 1948, Natural Evaporation from Open Water Bare Soil and Grass. Proc Roy Soc London, A193:120-145.
- Rachele, H., and A. Tunick, 1992, Estimating Effects of Temperature and Moisture of C_n^2 in the Damp Unstable Boundary Layer for Visible, Infrared, Radio and MM Wavelengths. In Proceedings of 1991 Battlefield Atmospheric Conference, El Paso, TX, 3-6 December 1991.
- Richardson, L. F., 1920, The Supply of Energy from and to Atmospheric Eddies. Proc Roy Soc, A97:354.
- Ritchie, J., 1972, Model for Predicting Evaporation from a Row Crop with Incomplete Cover. Water Res Resch, 8(5):1204-1213.
- Tetens, O., 1930, Uber Einige Meteorologische Begriffe. Z Geophysik, 6:297-309.

DISTRIBUTION LIST FOR PUBLIC RELEASE

Commandant
U.S. Army Chemical School
ATTN: ATSN-CM-CC (S. Barnes)
Fort McClellan, AL 36205-5020

NASA/Marshall Space Flight Center
Deputy Director
Space Science Laboratory
Atmospheric Sciences Division
ATTN: E501 (Dr. George Fichtl)
Huntsville, AL 35802

NASA/Marshall Space Flight Center
Atmospheric Sciences Division
ATTN: Code ED-41
Huntsville, AL 35812

Deputy Commander
U.S. Army Strategic Defense Command
ATTN: CSSD-SL-L (Dr. Lilly)
P.O. Box 1500
Huntsville, AL 35807-3801

Commander
U.S. Army Missile Command
ATTN: AMSMI-RD-AC-AD
(Mr. Peterson)
Redstone Arsenal, AL
35898-5242

Commander
U.S. Army Missile Command
ATTN: AMSMI-RD-AS-SS
(Huey F. Anderson)
Redstone Arsenal, AL
35898-5253

Commander
U.S. Army Missile Command
ATTN: AMSMI-RD-AS-SS
(B. Williams)
Redstone Arsenal, AL 35898-5253

Commander
U.S. Army Missile Command
ATTN: AMSMI-RD-DE-SE (Gordon Lill, Jr.)
Redstone Arsenal, AL 35898-5245

Commander
U.S. Army Missile Command
Redstone Scientific Information Center
ATTN: AMSMI-RD-CS-R/Documents
Redstone, Arsenal, AL 35898-5241

Commander
U.S. Army Intelligence Center and Fort Huachuca
ATTN: ATSI-CDC-C (Mr. Colanto)
Fort Huachuca, AZ 85613-7000

Northrup Corporation
Electronics Systems Division
ATTN: Dr. Richard D. Tooley
2301 West 120th Street, Box 5032
Hawthorne, CA 90251-5032

Commander - Code 3331
Naval Weapons Center
ATTN: Dr. Alexis Shlanta
China Lake, CA 93555

Commander
Pacific Missile Test Center
Geophysics Division
ATTN: Code 3250 (Terry E. Battalino)
Point Mugu, CA 93042-5000

Lockheed Missiles & Space Co.,
Inc.
Kenneth R. Hardy
Org/91-01 B/255
3251 Hanover Street
Palo Alto, CA 94304-1191

Commander
Naval Ocean Systems Center
ATTN: Code 54 (Dr. Juergen
Richter)
San Diego, CA 92152-5000

Meteorologist in Charge
Kwajalein Missile Range
P.O. Box 67
APO San Francisco, CA 96555

U.S. Department of Commerce
Center
Mountain Administration
Support Center, Library, R-51
Technical Reports
325 S. Broadway
Boulder, CO 80303

Dr. Hans J. Liebe
NTIA/ITS S 3
325 S. Broadway
Boulder, CO 80303

NCAR Library Serials
National Center for Atmos
Research
P.O. Box 3000
Boulder, CO 80307-3000

HQDA
ATTN: DAMI-POI
Washington, DC 20310-1067

Mil Asst for Env Sci Ofc of
The Undersecretary of Defense
for Resh & Engr/R&AT/E&LS
Pentagon - Room 3D129
Washington, DC 20301-3080

HQDA
DEAN-RMD/Dr. Gomez
Washington, DC 20314

Director
Division of Atmospheric Science
National Science Foundation
ATTN: Dr. Eugene W. Bierly
1800 G. Street, N.W.
Washington, DC 20550

Commander
Space & Naval Warfare
System Command
ATTN: FMW-145-1G (LT Painter)
Washington, DC 20362-5100

Commandant
U.S. Army Infantry
ATTN: ATSH-CD-CS-OR
(Dr. E. Dutoit)
Fort Benning, GA 30905-
5090

USAFETAC/DNE
Scott AFB, IL 62225

Air Weather Service
Technical Library - FL4414
Scott AFB, IL 62225-5458

USAFETAC/DNE
ATTN: Mr. Charles Glauber
Scott AFB, IL 62225-5008

Commander
U.S. Army Combined Arms Combat
ATTN: ATZL-CAW (LTC A. Kyle)
Fort Leavenworth, KS 66027-5300

Commander
U.S. Army Space Institute
ATTN: ATZI-SI
Fort Leavenworth, KS 66027-5300

Commander
U.S. Army Space Institute
ATTN: ATZL-SI-D
Fort Leavenworth, KS 66027-7300

Commander
Phillips Lab
ATTN: PL/LYP (Mr. Chisholm)
Hanscom AFB, MA 01731-5000

Director
Atmospheric Sciences Division
Geophysics Directorate
Phillips Lab
ATTN: Dr. Robert A.
McClatchey
Hanscom AFB, MA 01731-5000

Raytheon Company
Dr. Charles M. Sonnenschein
Equipment Division
528 Boston Post Road
Sudbury, MA 01776
Mail Stop 1K9

Director
U.S. Army Materiel Systems
Analysis Activity
ATTN: AMXSY-MP (H. Cohen)
APG, MD 21005-5071

Commander
U.S. Army Combined Arms Combat
ATTN: ATZL-CAW (LTC Kyle)
Fort Leavenworth, KS 66027-
5300

Director
ARL Chemical Biology
Nuclear Effects Division
ATTN: AMSRL-SL-CO
APG, MD 21010-5423

Director
U.S. Army Materiel Systems
Analysis Activity
ATTN: AMXSY-AT (Mr. Fred
Fred Campbell)
APG, MD 21005-5071

Director
U.S. Army Materiel Systems
Analysis Activity
ATTN: AMXSY-CR (Robert
M. Marchetti)
APG, MD 21005-5071

Director
Naval Research Laboratory
ATTN: Code 4110
(Mr. Lothar H. Ruhnke)
Washington, D.C. 20375-5000

Director
U.S. Army Materiel Systems
Analysis Activity
ATTN: AMXSY-CS (Mr. Bradley)
APG, MD 21005-5071

Director
U.S. Army Research Laboratory
ATTN: AMSRL-D
2800 Powder Mill Road
Adelphi, MD 20783-1145

Director
U.S. Army Research Laboratory
ATTN: AMSRL-OP-SD-TP
(Technical Publishing)
2800 Powder Mill Road
Adelphi, MD 20783-1145

Director
U.S. Army Research Laboratory
ATTN: AMSRL-OP-CI-SD-TL
2800 Powder Mill Road
Adelphi, MD 20783-1145

Director
U.S. Army Research Laboratory
ATTN: AMSRL-SS-SH
(Dr. Z.G. Sztankay)
2800 Powder Mill Road
Adelphi, MD 20783-1145

National Security Agency
ATTN: W21 (Dr. Longbothum)
9800 Savage Road
Fort George G. Meade, MD
20755-6000

U.S. Army Space Technology
and Research Office
ATTN: Brenda Brathwaite
5321 Riggs Road
Gaithersburg, MD 20882

Commander
U.S. Army Aviation Center
ATTN: ATSQ-D-MA (Mr. Heath)
Fort Rucker, AL 36362
OIC-NAVSWC
Technical Library (Code E-232)
Silver Springs, MD 20903-5000

Director
Naval Research Laboratory
ATTN: Code 4110
(Dr. Lothar H. Ruhnke)
Washington, D.C. 20375-5000

Commander
U.S. Army Research Office
ATTN: DRKRO-GS (Dr. W.A.
Flood) P.O. Box 12211
Research Triangle Park, NC
27009

Dr. Jerry Davis
North Carolina State
University
Department of Marine, Earth,
& Atmospheric Sciences
P.O. Box 8208
Raleigh, NC 27650-8208

Commander
U. S. Army CECRL
ATTN: CECRL-RG (Dr. Boyne)
Hanover, NH 03755-1290

Commanding Officer
U.S. Army ARDEC
ATTN: SMCAR-IMI-I, Bldg 59
Dover, NJ 07806-5000

Commander
U.S. Army Communications-
Electronics Center for
EW/RSTA
ATTN: AMSEL-RD-EW-SP
Fort Monmouth, NJ 07703-5206

Commander
U.S. Army Satellite Comm
Agency
ATTN: DRCPM-SC-3
Fort Monmouth, NJ 07703-5303

Commander
U.S. Army Dugway Proving Ground
ATTN: STEDP-MT-DA-L
Dugway, UT 84022-5000

Commander
U.S. Army Satellite Comm Agency
ATTN: DRCPM-SC-3
Fort Monmouth, NJ 07703-5303

HQ AWS/DOO
Scott AFB, IL 62225-5008

Commander
Department of the Air Force
OL/A 2d Weather Squadron (MAC)
Holloman AFB, NM 88330-5000

PL/WE
Kirtland AFB, NM
87118-6008

Director
U.S. Army TRADOC Analysis Center
ATTN: ATRC-WSS-R
White Sands Missile Range, NM
88002-5502

USAF Rome Laboratory Technical
Library, FL2810
Corridor W, STE 262, RL/SUL
26 Electronics Parkway, Bldg 106
Griffiss AFB, NY 13441-4514

AFMC/DOW
Wright-Patterson AFB, OH
0334-5000

Commandant
U.S. Army Field Artillery School
ATTN: ATSF-TSM-TA (Mr. Taylor)
Fort Sill, OK 73503-5600

Commander
Naval Air Development Center
ATTN: Al Salik (Code 5012)
Warminster, PA 18974

Commander
U.S. Army Dugway Proving Ground
ATTN: STEDP-MT-M (Mr. Bowers)
Dugway, UT 84022-5000

Defense Technical Information
Center
ATTN: DTIC-OCF (2)
Cameron Station
Alexandria, VA 22314-6145

Commanding Officer
U.S. Army Foreign Science &
Technology Center
ATTN: CM
220 7th Street, NE
Charlottesville, VA 22901-5396

Naval Surface Weapons Center
Code G63
Dahlgren, VA 22448-5000

Commander
U.S. Army OEC
ATTN: CSTE-EFS
Park Center IV
4501 Ford Ave
Alexandria, VA 22302-1458

Commander and Director
U.S. Army Corps of Engineers
Engineer Topographics Laboratory
ATTN: ETL-GS-LB
Fort Belvoir, VA 22060

TAC/DOWP
Langley AFB, VA 23665-5524

U.S. Army Topo Engineering Center
ATTN: CETEC-ZC
Fort Belvoir, VA 22060-5546

Commander
Logistics Center
ATTN: ATCL-CE
Fort Lee, VA 23801-6000

Commander
USATRADOCC
ATTN: ATCD-FA
Fort Monroe, VA 23651-5170

Science and Technology
101 Research Drive
Hampton, VA 23666-1340

Commander
U.S. Army Nuclear & Cml
Agency
ATTN: MONA-ZB, Bldg 2073
Springfield, VA 22150-3198

Commander
U.S. Army Communications-
Electronics Center for EW/RSTA
ATTN: AMSEL-EW-D (File Copy)
Fort Monmouth, NJ 07703-5303

Commander
U.S. Army Communications-
Electronics Center for EW/RSTA
ATTN: AMSEL-EW-MD
Fort Monmouth, NJ 07703-5303

Commander
U.S. Army Field Artillery School
ATTN: ATSF-F-PD (Mr. Gullion)
Fort Sill, OK 73503-5600